A Magnitude/Phase Locked Loop Approach to Parameter Estimation of Periodic Signals

Biqing Wu and Marc Bodson*

Abstract: The paper presents a parameter estimator that is designed to estimate the frequencies, magnitudes, and phases of the components of a periodic signal. The structure of the algorithm is reminiscent of a phase-locked loop, although significant differences can be observed. The performance of the estimator is analyzed, and useful design guidelines are provided. A version of the algorithm is presented that combines different components of the signal, and/or signals from multiple sensors, in order to estimate the fundamental frequency. In this manner, the algorithm is able to maintain tracking of the fundamental frequency despite changes in signal characteristics. The results are verified in simulations, and the algorithms are found to be simple and effective for estimation and tracking of time-varying parameters. Experimental results are reported where periodic signals are collected from an active noise control testbed.

1. Introduction

The estimation of the parameters (*e.g.,* frequencies, magnitudes, and phases) of periodic signals buried in noise is important in many practical applications of signal processing, system identification and control system design. To estimate the frequencies, several approaches exist, among others: (1) the classical non-parametric power spectral estimation [7]; (2) eigen-analysis (or subspace tracking) spectrum estimation [13], [16]; (3) extended Kalman filter frequency estimation [2], [8]; (4) adaptive notch filtering [1], [6], [9], [10], [11], [12], [14]; and (5) the phase-locked loop [5].

Power spectral estimation has the problem of spectral leakage due to windowing, and the resolution of the frequency estimate is poor for time-varying applications. The eigen-analysis works well for high signal-noise-ratio (SNR) and is suitable for communication applications and in sensor array processing. Extended Kalman filtering is most suitable in nonstationary situations. Both eigen-analysis and extended Kalman filtering suffer from demanding computational requirements. For control system applications, such as in active control of narrowband acoustic noise, on-line implementation requires computational efficiency, good stability properties, and fast convergence. Frequency estimation based on adaptive notch filtering is often preferred. Still, it is a complex task to analyze the performance of an adaptive notch filter, and the stability is not always guaranteed.

This paper presents a frequency estimator based on a new *magnitude/phase locked loop* approach. As the name indicates, the scheme is similar to a phase-locked loop, but a major difference is that the magnitude and the frequency of the incoming signal are estimated simultaneously. Overall, the estimator has the following features:

*This material is based upon work supported by the National Science Foundation under Grant No. ECS0115070.

simultaneous estimation of the frequencies, magnitudes and phases of the components of a periodic signal, simplicity in design and implementation, and fast estimation/tracking of time-varying parameters. Preliminary versions of the results were presented in [18] and [19].

The algorithm is derived from the "direct" disturbance rejection algorithm presented in [4], with an adjustment made to improve frequency tracking. The performance analysis of the algorithm using the approximation of [4] is accurate when the system states are close to the equilibrium, but a desire to guarantee convergence for large initial frequency error justifies a more advanced study of the nonlinear behavior of the parameter estimation algorithm, which is presented in the paper. Some design guidelines are given to ensure the desired performance of the frequency estimation loop, in terms of convergence time and in terms of variance of the estimate in the presence of noise.

The algorithm extracts frequency information from the fundamental component of the signal. A modified version of the algorithm is also presented, in which harmonics contribute to the fundamental frequency estimation. The extension is useful for situations in which the fundamental component of the signal may become small, or even vanish for some periods of time. Similarly, multiple signals with the same fundamental frequency can also be combined to yield better frequency estimation results.

2. Basic Adaptive Algorithm

2.1 Description of the Algorithm

Fig. 1 shows a graphical representation of the algorithm. For simplicity of presentation, the periodic signal is assumed to contain only the fundamental and the third harmonic, so that

$$d(t) = m_{1d}\cos\left(\alpha_{1d}(t)\right) + m_{3d}\cos\left(\alpha_{3d}(t)\right), \tag{1}$$

The phase angles satisfy

$$\dot{\alpha}_{1d} = \omega_d,\ \alpha_{1d}(0) = \alpha_{10},\ \dot{\alpha}_{3d} = 3\omega_d,\ \alpha_{3d}(0) = \alpha_{30}. \tag{2}$$

The unknown parameters are the magnitudes m_{1d}, m_{3d}, the frequency ω_d, and the phase parameters α_{10}, α_{30}.

Variables m_1, α_1, m_3 and α_3 are defined to be estimates of the magnitudes and phases of the two components of the signal, respectively. ω is the estimate of the fundamental frequency. ϕ_3 is defined as the estimate of the "relative" phase of the third harmonic, that is $\phi_3 = \alpha_3 - 3\alpha_1$. Finally, the signal $\hat{d}(t)$ is the estimate of the incoming periodic signal $d(t)$. The equations for the adaptive algorithm shown in Fig. 1 are:

$$\begin{aligned}
\hat{d}(t) &= m_1(t)\cos\left(\alpha_1(t)\right) + m_3(t)\cos\left(\alpha_3(t)\right),\ \alpha_1(t) = K_f\,\omega(t) + \int_0^t \omega(\tau)d\tau, \\
\dot{m}_1(t) &= 2g_m\left(d(t) - \hat{d}(t)\right)\cos\left(\alpha_1(t)\right),\ \dot{m}_3(t) = 2g_m\left(d(t) - \hat{d}(t)\right)\cos\left(\alpha_3(t)\right), \\
\dot{\omega}(t) &= -2g_\omega\left(d(t) - \hat{d}(t)\right)\sin\left(\alpha_1(t)\right),\ \dot{\phi}_3(t) = -2g_\phi\left(d(t) - \hat{d}(t)\right)\sin\left(\alpha_3(t)\right),
\end{aligned} \tag{3}$$

where the design parameters K_f, g_m, g_ω, and g_ϕ are all positive. The algorithm has four adaptive parameters, whose nominal values are $\omega^* = \omega_d$, $\phi_3^* = \alpha_{30} - 3\alpha_{10}$, $m_1^* = m_{1d}$, and $m_3^* = m_{3d}$. The algorithm developed initially from the results of [4] used $K_f = 0$, which is more intuitive since the phase α_1 becomes the integral of the fundamental frequency. The stability analysis, however, shows that $K_f > 0$ improves the dynamic response of the algorithm and simplifies its design.

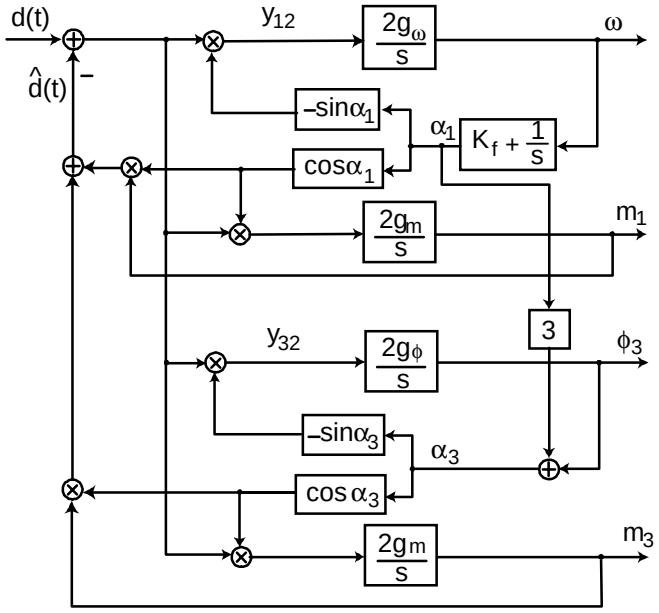

Figure 1: Parameter estimator for a signal with a fundamental and a third harmonic

The scheme can easily be extended to periodic signals with arbitrary number of harmonic components by adding one magnitude estimation loop and one relative phase estimation loop (such as these yielding m_3 and ϕ_3) for every additional harmonic. A similar algorithm can also be developed by replacing the differential equations by difference equations, and performing the analysis in the discrete-time domain (see [3] for an application to a simplified algorithm). Here, the frequency estimator is developed and analyzed in continuous-time. Simulations are carried out using an Euler approximation of the continuous-time algorithm and confirm the analysis.

2.2 Frequency Estimation Loop: Linear Analysis

The frequency loop of the algorithm is similar to a phase-locked loop (PLL). However, there is one aspect that makes the loop significantly different from a standard PLL: the reconstructed signal is subtracted from the incoming signal. One consequence is that the magnitude as well as the frequency and phases of the incoming signal can be estimated with this scheme. Another difference is that the error signal goes to zero when the parameters converge to their nominal values, so that the frequency estimate converges exactly to the nominal value in the ideal case (in other words, the steady-state frequency estimate is free from the ripple that is observed in PLL's).

As for phase-locked loops, useful results are obtained by discarding high frequency terms at the output of the multipliers. We assume that the frequency estimate ω is close enough to the fundamental frequency ω_d for the approximation to be valid. In this manner, we have:

$$y_{12} \simeq -\frac{1}{2} m_{1d} \sin(\alpha_1 - \alpha_{1d}). \tag{4}$$

The discarding of the high-frequency components is justified by the low-pass property of the filter $2g_\omega/s$. An additional low-pass filter may be added, but simulations show that it is not needed for the satisfactory operation of the estimator. Notice from equation (4) that the frequency loop is independent of the other three loops after the high-frequency terms were discarded, which is useful for the analysis.

Defining the phase and frequency estimation errors $\tilde{\alpha}_1 = \alpha_1 - \alpha_{1d}$ and $\tilde{\omega} = \omega - \omega_d$, the differential equations

that describe the frequency loop are then

$$\frac{d\tilde{\alpha}_1}{dt} = \tilde{\omega} - g_\omega m_{1d} K_f \sin(\tilde{\alpha}_1), \ \frac{d\tilde{\omega}}{dt} = -g_\omega m_{1d} \sin(\tilde{\alpha}_1) - \dot{\omega}_d, \tag{5}$$

The above equations are nonlinear, autonomous, and second-order. A linearized system can be obtained when the parameters are close to their nominal values and the phase error $\tilde{\alpha}_1$ is small. The linear dynamics of the loop are then those of a second-order system with poles determined by the roots of $s^2 + g_\omega m_{1d} K_f s + g_\omega m_{1d} = 0$. Stability is guaranteed as both coefficients are positive. With constant ω_d, the frequency estimate ω and the phase estimate α_1 converge to their nominal values in the steady-state. If the frequency of the incoming signal is increasing linearly, *i.e.,* $\dot{\omega}_d$ is constant, $\tilde{\omega}$ and $\tilde{\alpha}_1$ converge to $-\dot{\omega}_d K_f$ and $-\dot{\omega}_d/(g_\omega m_{1d})$, respectively.

2.3 Frequency Estimation Loop: Nonlinear Analysis and Convergence Time

The nonlinear behavior of the frequency estimation loop may be studied using a technique similar to the one found in [15] pp.124-133. Assuming that the frequency of the incoming signal is fixed, *i.e.,* $\dot{\omega}_d = 0$, for the differential equations (5), the trajectories of $(\tilde{\alpha}_1, \tilde{\omega})$ converge to $(n\pi, 0)$ with n an even integer, except the rarely-happening hang-up at saddle points with n odd. This result implies that the frequency estimate ω converges to ω_d. When the incoming signal contains only one sinusoid, the convergence occurs with an infinite pull-in range. Local stability is guaranteed for multiple sinusoids. In that case, one must have an initial estimate that is close to the fundamental frequency of the signal, to make sure that the frequency estimate locks on the fundamental frequency instead of a harmonic frequency.

In practical situations, the convergence time may be very long for large initial frequency error, so that it is useful to determine the relationship between the convergence time and the design parameters in order to achieve desirable performance. Because of the nonlinearity of the system, it is difficult to determine an exact formula, but two limiting cases can be analyzed.

Case 1: $g_\omega m_{1d} K_f$ **small:** a method similar to the one used in [15] pp.161-168 can be followed, assuming that $g_\omega m_{1d} K_f$ is small compared to the initial frequency estimation error $\tilde{\omega}(0) = \omega(0) - \omega_d(0)$. Then, the loop will slip a certain number of cycles before locking up, and the pull-in time is approximately given by

$$T_d \simeq \frac{\tilde{\omega}^2(0)}{(g_\omega m_{1d})^2 K_f}, \tag{6}$$

which is proportional to the square of the initial frequency error. The estimator converges very fast after the system enters the lock-in region, as K_f is small (the convergence time for the system in the lock-in region will be shown in Case 2). Note that the convergence time decreases with increasing values of $g_\omega m_{1d}$ and K_f.

Case 2: $g_\omega m_{1d} K_f$ **large:** when $g_\omega m_{1d} K_f$ is large compared to $\tilde{\omega}(0)$, there is no cycle slipping and the system enters the lock-in region right away. The convergence time is found to be $T_d = K_f \ln(\tilde{\omega}(0) - \ln \tilde{\omega}_\infty)$, where the frequency estimation error $\tilde{\omega}_\infty$ is a small value defining when convergence is achieved. The convergence time T_d in this situation does not depend on the value of g_ω or m_{1d}, and increases with K_f.

When $g_\omega m_{1d} K_f$ is close to $\tilde{\omega}(0)$, the convergence time may be determined by the combination of the above two limiting cases. If $g_\omega m_{1d}$ is fixed, the convergence time T_d will decrease when K_f increases, as in case 1; T_d will also decrease when K_f decreases, as in case 2. In both cases, T_d will decrease when $g_\omega m_{1d} K_f$ comes closer to $\tilde{\omega}(0)$. If

K_f is fixed, T_d will decrease with the increase of $g_\omega m_{1d}$, as in case 1. When $g_\omega m_{1d}$ is increased to such value that $g_\omega m_{1d} K_f$ is large compared to $\tilde{\omega}(0)$, T_d stays at some value for a fixed K_f, as in case 2. So, it may be assumed that a good design of the parameters g_ω and K_f is to make $g_\omega m_{1d} K_f$ close to $\tilde{\omega}(0)$. In practical situations, the usefulness of the result is limited by the fact that the initial frequency error $\tilde{\omega}(0)$ and the magnitude m_{1d} are not known. However, in most cases, some prior knowledge about the value of $\tilde{\omega}(0)$ and m_{1d} is available, and can be used to choose the parameters K_f and g_ω such that the convergence time T_d is satisfactory.

2.4 Frequency Estimation Loop: Noise Sensitivity

Usually, the periodic signal is corrupted by measurement noise $n(t)$, whose effect may be analyzed under the assumption that the noise is white with variance σ^2. The incoming signal is assumed to be given by:

$$d(t) = m_{1d} \cos(\alpha_{1d}(t)) + m_{3d} \cos(\alpha_{3d}(t)) + n(t), \tag{7}$$

The output of the multiplier in the frequency estimation loop is, discarding high frequency terms as before

$$y_{12}(t) = -\frac{1}{2} m_{1d} \sin(\alpha_1(t) - \alpha_{1d}(t)) + n_s(t), \;\; n_s(t) = n(t) \sin(\alpha_1(t)) \,. \tag{8}$$

In the noise analysis of phase-locked loops, one typically assumes that n_s is a white noise with variance equal to $\sigma^2/2$. The variance of the frequency estimate of the signal can then be found to be:

$$\sigma_\omega^2 = \frac{g_\omega \sigma^2}{m_{1d} K_f}. \tag{9}$$

While convergence time can be reduced by increasing g_ω, there is an expected trade-off between convergence time and noise sensitivity, and the above formulas can be used to choose a desirable setting of the design parameters.

2.5 Magnitude and Phase Estimation Loops

After the frequency loop converges, the other three parameter estimation loops can be approximated as independent subsystems. The approximate systems for the estimation of the magnitude of the fundamental, the magnitude of the 3rd harmonic, and the relative phase are respectively given by:

$$\begin{aligned}
\dot{m}_1 &= -g_m \left(m_1 - m_{1d} \cos(\alpha_1 - \alpha_{1d})\right) \simeq -g_m (m_1 - m_{1d}), \\
\dot{m}_3 &= -g_m \left(m_3 - m_{3d} \cos(\alpha_3 - \alpha_{3d})\right) \simeq -g_m (m_3 - m_{3d}), \\
\dot{\phi}_3 &= -g_\phi m_{3d} \sin(\phi_3 - \phi_3^*) \simeq -g_\phi m_{3d} (\phi_3 - \phi_3^*),
\end{aligned} \tag{10}$$

where the second set of equations applies when α_1, α_3, and ϕ_3 are close to α_{1d}, α_{3d}, and ϕ_3^*. The dynamics of m_1 and m_3 are first-order, with poles at $s = -g_m$. The dynamics of ϕ_3 are also those of a first-order linear system, with a pole at $-g_\phi m_{3d}$. When the fundamental frequency of the incoming signal is constant, the phase estimation errors become zero in the steady-state, and the magnitude estimates converge to their nominal values.

3. Simulation Results

3.1 Validation of Analysis: Varying g_ω for Fixed K_f

The validity of the prediction of the convergence time and of the noise sensitivity was examined via simulation. An Euler approximation of the continuous-time algorithm was used with a sampling frequency of $f_s = 1000$ Hz.

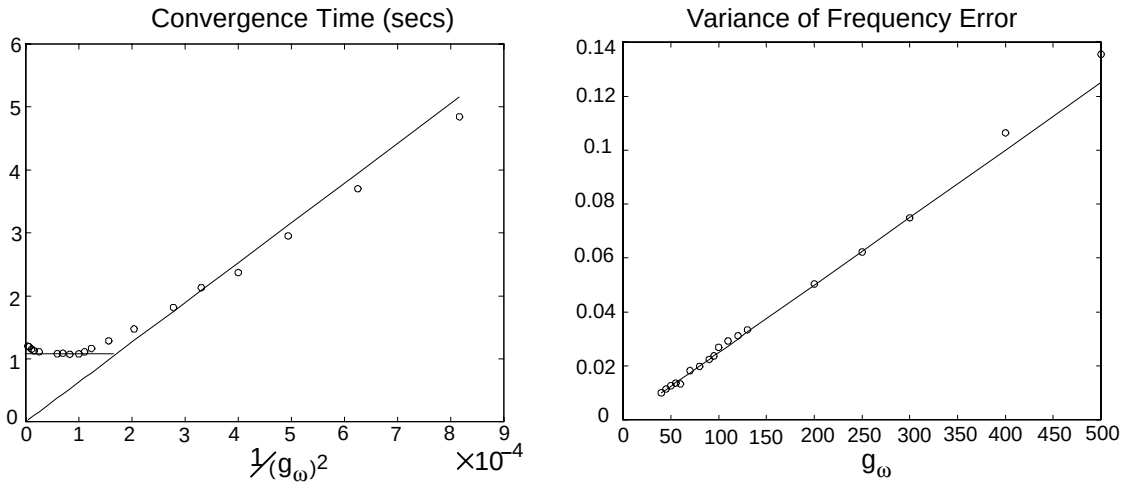

Figure 2: Convergence time and variance of frequency error as functions of g_ω (predicted *vs.* simulation)

The phase estimates α_1 and α_3 were reset to the range $[0,\ 2\pi]$ when new estimates exceeded that range. The input signal contained white noise with variance of $\sigma^2 = 0.01^2$ (which corresponds to a discrete-time sequence with variance equal to $0.01^2/T_s$, where $T_s = 1/f_s$), leading to a signal to noise ratio of 10 dB. The convergence time and the variance of the frequency estimate were computed for different values of g_ω and fixed $K_f = 0.4$. The convergence time versus $(1/g_\omega)^2$ is shown in the left of Fig. 2, where the solid line is the predicted convergence time, and the circles are the convergence times obtained from the simulation. One finds that when g_ω is small and $g_\omega m_{1d} K_f < \tilde{\omega}(0)$, the convergence time is satisfactorily approximated by $T_d = \tilde{\omega}^2(0)/(g_\omega m_{1d})^2 K_f$. Increasing the value of g_ω will not decrease the convergence time indefinitely. Instead the convergence time has a lower limit, which is given by constant $T_d = -K_f(\ln \tilde{\omega}_\infty - \ln \tilde{\omega}(0))$ for fixed K_f (horizontal line in the figure).

Fig. 2 on the right shows the variance error of the frequency estimate versus g_ω. Again, the solid line is the estimated value, and the circles are the ones obtained from the simulation. The match between the actual variance errors and the predicted values is good. Similar to any other adaptive algorithm, the choice of step size g_ω is a trade-off between short convergence time and small variance error, up to the point where g_ω becomes too large and the convergence time reaches the lower limit determined by the value of K_f.

3.2 Validation of Analysis: Varying K_f for Fixed g_ω

Fig. 3 shows the convergence time and the variance error of the frequency estimate versus $1/K_f$, for different values of K_f and fixed $g_\omega = 80$. The solid line gives the predicted values, and the circles are the values obtained from the simulation. Fig. 3 on the left shows that the convergence time is approximated by $T_d = \tilde{\omega}^2(0)/(g_\omega m_{1d})^2 K_f$ for small K_f, and by $T_d = -K_f(\ln \tilde{\omega}_\infty - \ln \tilde{\omega}(0))$ for large K_f. The match between the predicted values and those obtained from the simulation is good. The simulation results show that the performance analysis is precise, although it ignores the high frequency components of the signals originating from the multipliers. Also, the steady-state bias of the frequency estimate is virtually zero, although more than one sinusoidal component exists in the incoming signal.

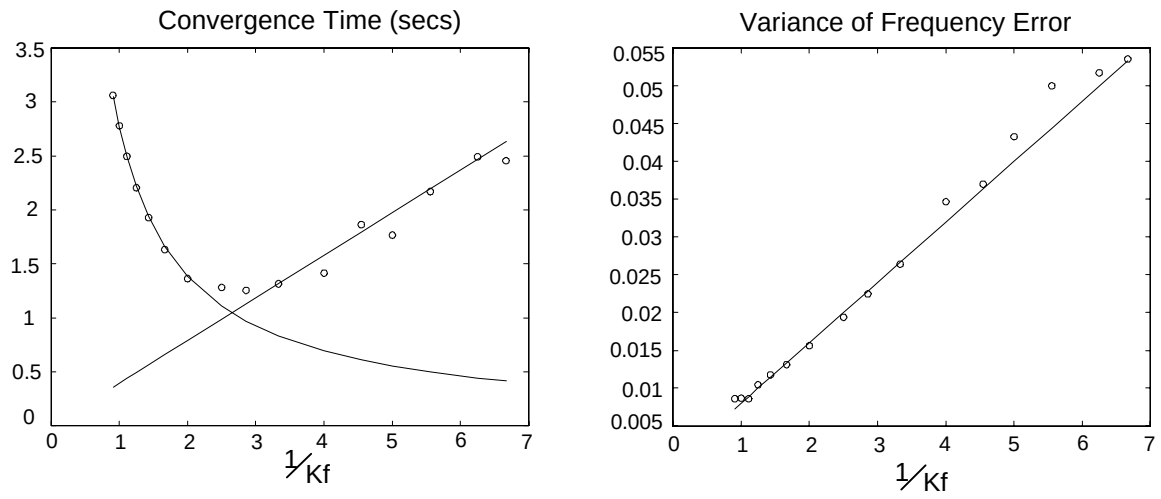

Figure 3: Convergence time and variance of frequency error as functions of K_f (predicted *vs.* simulation)

4. Modified Frequency Estimator

4.1 Combination of Different Components

In Section 2, frequency estimation was solely based on the fundamental component, which was assumed to be the largest component of the signal. However, in some situations, the magnitude of the fundamental component may become low, while the magnitudes of the harmonics remain significant. It is then beneficial to extract the frequency information from all the components of the periodic signal. A modification of the parameter estimator is proposed that enable multiple harmonics of a signal to contribute to the estimation.

Fig. 4 shows the modified algorithm. The part of the scheme responsible for the estimation of the magnitudes is the same as in the original parameter estimator illustrated by Fig. 1 (called the *basic* algorithm hereafter). The equations for the frequency and phase estimation are now, assuming $N = 3$,

$$\begin{aligned}
\alpha_1(t) &= K_f\omega_1(t) + \int_0^t \omega(\tau)d\tau,\ \alpha_3(t) = K_f\phi_3(t) + N\int_0^t \omega(\tau)d\tau, \\
y_{12}(t) &= -\left(d(t) - \hat{d}(t)\right)\sin\left(\alpha_1(t)\right),\ y_{32}(t) = -\left(d(t) - \hat{d}(t)\right)\sin\left(\alpha_3(t)\right), \\
\dot{\omega}_1(t) &= 2g_\omega y_{12}(t),\ \dot{\phi}_3(t) = 2g_\phi y_{32}(t),\ \omega(t) = \omega_1(t) + \frac{1}{N}\phi_3(t),
\end{aligned} \tag{11}$$

The design parameters K_f, g_ω, and g_ϕ are similar to those in the basic parameter estimator, and N is the number of the harmonic, which is 3 for this presentation. Similarly, the nominal value of the fundamental frequency estimate ω is $\omega^* = \omega_d$, and the parameters α_1, and α_3 have nominal values $\alpha_1^* = \alpha_{1d}$ and $\alpha_3^* = \alpha_{3d}$, respectively. However, the nominal value for ϕ_3 is given by $\phi_3^* = \left(\alpha_{3d}(0) - N\alpha_{1d}(0)\right)/(2K_f) + N\omega_d/2$, which is not the same as in the previous parameter estimator. Overall, there is a slight, but marginal increase of computational complexity in the modified algorithm, compared to the basic algorithm shown in Fig. 1.

Again, discarding the high frequency terms at the output of the multipliers and assuming that the parameters are close to their nominal values, a linear approximation can be found. The analysis shows that the system is always stable if the design parameters are positive. When the fundamental frequency of the incoming signal is constant, the frequency estimate ω and the phase estimate α_1 converge to their nominal values. An interesting

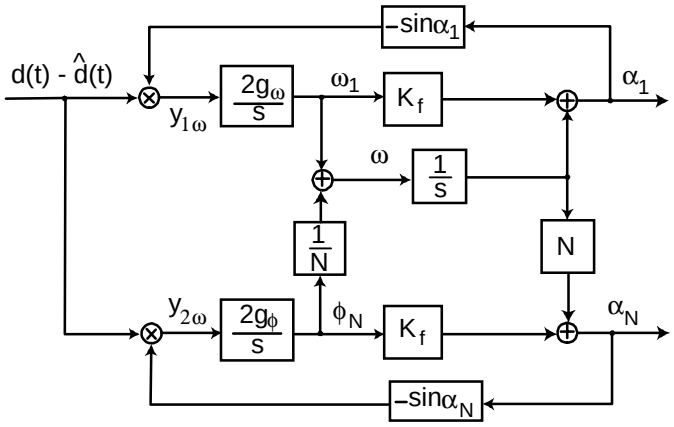

Figure 4: Modified frequency estimator

feature of the modified algorithm is observed when one of the two components of the incoming signal does not exist. Then, the frequency estimator reduces to the basic parameter estimator that is based on the non-zero component of the signal. Noise sensitivity analysis shows that the noise variance is finite as long as one of the components of the incoming signal is present. In the basic parameter estimator, the variance of the frequency estimate was given by equation (9), which becomes infinite if the fundamental component does not exist. Details of this analysis are available in [17].

4.2 Combination of Different Signals

The frequency estimator shown in Fig. 4 can be modified to include components from two different signals. In this case, the variables $y_{1\omega}$ and $y_{2\omega}$ in Fig. 4 are obtained from the two signals, instead of from two harmonics of a single signal. The number N can be any integer that indicates which component of the second signal is combined in the frequency estimator. Further, the scheme can be extended so that an arbitrary number of components and/or signals may be combined to contribute to the fundamental frequency estimation.

In general, we assume L incoming signals $d_1(t)$, $d_3(t)$, ..., $d_L(t)$, each of which contains I components. In the following definitions, $i = 1, 2, ..., I$, $l = 1, 2, ..., L$. Define the variables $y_{l,is} = (d_l - \hat{d}_l)(-\sin(\alpha_{l,i}))$, where $\hat{d}_l$ are the corresponding estimated signals, and $\alpha_{l,i}$ represents the estimated phase of the i^{th} component of the l^{th} signal. The variables $y_{l,ic}$ are defined to be $y_{l,ic} = (d_l - \hat{d}_l)\cos(\alpha_{l,i})$. To describe the modified parameter estimator in a compact form, we define the vectors

$$\begin{aligned} \mathbf{Y}_s &= \begin{bmatrix} \mathbf{Y}_{1s}^T & \mathbf{Y}_{2s}^T & ... & \mathbf{Y}_{Is}^T \end{bmatrix}^T, \ \mathbf{Y}_c = \begin{bmatrix} \mathbf{Y}_{1c}^T & \mathbf{Y}_{2c}^T & ... & \mathbf{Y}_{Ic}^T \end{bmatrix}^T, \\ \mathbf{Y}_{is} &= \begin{bmatrix} y_{1,is} & y_{2,is} & ... & y_{L,is} \end{bmatrix}^T, \ \mathbf{Y}_{ic} = \begin{bmatrix} y_{1,ic} & y_{2,ic} & ... & y_{L,ic} \end{bmatrix}^T \end{aligned} \tag{12}$$

We also define the corresponding estimated magnitude and phase vectors

$$\begin{aligned} \mathbf{m} &= \begin{bmatrix} \mathbf{m}_1^T & \mathbf{m}_2^T & ... & \mathbf{m}_I^T \end{bmatrix}^T, \ \boldsymbol{\phi} = \begin{bmatrix} \boldsymbol{\phi}_1^T & \boldsymbol{\phi}_2^T & ... & \boldsymbol{\phi}_I^T \end{bmatrix}^T, \\ \mathbf{m}_i &= \begin{bmatrix} m_{1,i} & m_{2,i} & ... & m_{L,i} \end{bmatrix}^T, \ \boldsymbol{\phi}_i = \begin{bmatrix} \phi_{1,i} & \phi_{2,i} & ... & \phi_{L,i} \end{bmatrix}^T \end{aligned} \tag{13}$$

The magnitude and phase estimates are updated according to $\dot{\mathbf{m}} = 2\mathbf{g}_m\mathbf{Y}_c$, $\dot{\boldsymbol{\phi}} = 2\mathbf{g}_\omega\mathbf{Y}_s$, where diagonal matrices

$\mathbf{g}_m$ and $\mathbf{g}_\omega$ are given by

$$\begin{aligned} \mathbf{g}_m &= diag\ (g_{1,1m}\ g_{2,1m}\ \cdots\ g_{L,1m}\ \cdots\ g_{1,Im}\ g_{2,Im}\ \cdots\ g_{L,Im}), \\ \mathbf{g}_\omega &= diag\ (g_{1,1\omega}\ g_{2,1\omega}\ \cdots\ g_{L,1\omega}\ \cdots\ g_{1,I\omega}\ g_{2,I\omega}\ \cdots\ g_{L,I\omega}). \end{aligned} \tag{14}$$

The frequency estimate is obtained by

$$\omega = \left[\begin{array}{cccccccccccc} 1 & 1 & ... & 1 & 1/2 & 1/2 & ... & 1/2 & ... & 1/I & 1/I & ... & 1/I \end{array} \right] \boldsymbol{\phi}. \tag{15}$$

Defining the vector containing the phases of the components of the signals

$$\boldsymbol{\alpha} = \left[\begin{array}{cccc} \boldsymbol{\alpha}_1^T & \boldsymbol{\alpha}_2^T & ... & \boldsymbol{\alpha}_I^T \end{array} \right]^T, \ \boldsymbol{\alpha}_i = \left[\begin{array}{cccc} \alpha_{1,i} & \alpha_{2,i} & ... & \alpha_{L,i} \end{array} \right]^T \tag{16}$$

such that

$$\boldsymbol{\alpha} = \left[\begin{array}{cccccccccccc} 1 & 1 & ... & 1 & 2 & 2 & ... & 2 & ... & I & I & ... & I \end{array} \right]^T \alpha_0 + K_f \boldsymbol{\phi},\ \dot{\alpha}_0 = \omega. \tag{17}$$

If the elements of the matrix $\mathbf{g}_\omega$ are chosen such that,

$$g_{1,1\omega} m_{1,1d} = g_{2,1\omega} m_{2,1d} = ... = g_{L,1\omega} m_{L,1d} = ... = g_{1,I\omega} m_{1,Id} = ... = g_{L,I\omega} m_{L,Id} = K, \tag{18}$$

the characteristic equation for the frequency estimator is given by

$$(s + K\ K_f)^{N-1} (s^2 + K\ K_f s + JK\ ) = 0, \tag{19}$$

where J is the total number of the components that are included in the fundamental frequency estimation. The characteristic equation shows that, with this choice, the system is stable for all positive values of K_f and K. The dynamics of the magnitude estimates are decoupled and first-order, with poles at $s = -g_{l,im}$ for $m_{l,i}$.

The combination of the components of different signals in the fundamental frequency estimation makes the estimator more flexible, as it is not necessary to know *a priori* which components exist or which component is the most suitable to base the frequency estimation on. The modified algorithm is especially useful when the magnitudes of the components of the signals change significantly with time.

5. Simulation and Experimental Results

5.1 Simulation Results

A comparison between the basic and the modified estimators was performed via a simulation. In the simulation, the periodic signal was chosen to contain a fundamental and a 2nd harmonic, with the fundamental frequency increasing linearly from 148 Hz to 176 Hz in 3.5 seconds. The simulation was designed to illustrate a rather extreme case where the magnitude of the fundamental completely vanished for some period of time (between 1 and 1.5 seconds in the experiment). The measurement noise contained in the signal was set to be white noise with variance of 0.01. The sampling frequency is set to $f_s = 2000$ Hz.

Fig. 5, on the left, shows the frequency tracking performance of the basic parameter estimator. The basic parameter estimator is not able to track the changing frequency of the signal when the magnitude of the fundamental

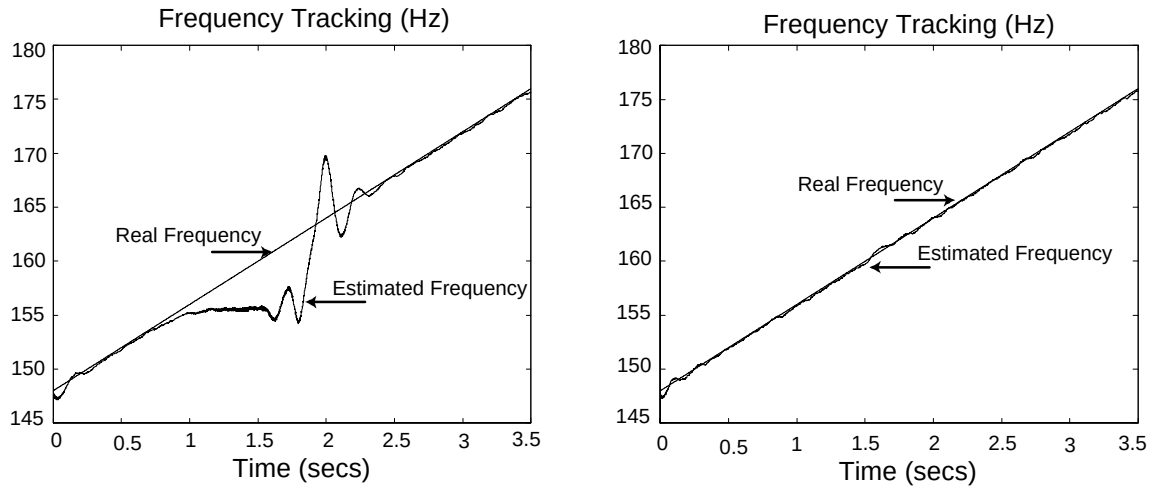

Figure 5: Frequency tracking of the basic estimator (left) and modified estimator (right)

component becomes zero. Fig. 5, on the right, shows that the modified parameter estimator tracks consistently the frequency of the signal. The modified parameter estimator has better stability properties and tracking performance than the original estimator at the cost of only a slight increase in computational complexity.

5.2 Experimental Results

The performances of the modified frequency estimator was also investigated with experimental data. The incoming signals were obtained from an active noise control testbed. The testbed consisted in a Motorola's DSP96002 32-bit floating-point digital signal processor hosted in a PC, microphones, and bookshelf speakers with a 4-inch low-frequency driver. For the experiments of this paper, one of the speakers generated a periodic signal constituting the noise source. The signals were collected by two microphones about 2.7 ft apart. These signals were passed through an anti-aliasing filter and sampled by a self-calibrating 16-bit analog-to-digital converter before being recorded by the DSP system. The sampling frequency $f_s = 2000$ Hz. The incoming signals, shown on the left of Fig. 6, were collected by the two microphones when a sound wave with a fundamental and a 2nd harmonic was produced by the loudspeaker. The amplitudes of the source signal were fixed, while the fundamental frequency increased linearly from $100Hz$ to $220Hz$ in 10 seconds. Due to the acoustic properties of the room, the amplitudes of the components of the signal collected by the microphone rapidly changed with the frequency. At some frequencies, the fundamental was very small.

Fig. 6 on the right shows the frequency tracking performance of the modified parameter estimator with $L = 2$ and $I = 2$, *i.e.*, both components of the two signals were used in the fundamental frequency estimation. The design parameters for magnitude estimation $g_{l,im}$ with $l = 1, 2$ and $i = 1, 2$ were all set to 20. The design parameter K_f was set to 0.06, and $g_{l,i\omega}$ with $l = 1, 2$ and $i = 1, 2$ all to 6000. The modified parameter estimator is found to track the changing frequency of the signal consistently throughout the experiment.

6. Conclusions

In this paper, a magnitude/phase-locked loop parameter estimator was proposed which simultaneously estimated the frequencies, magnitudes and phases of the sinusoidal components of a signal. The signal was assumed to contain

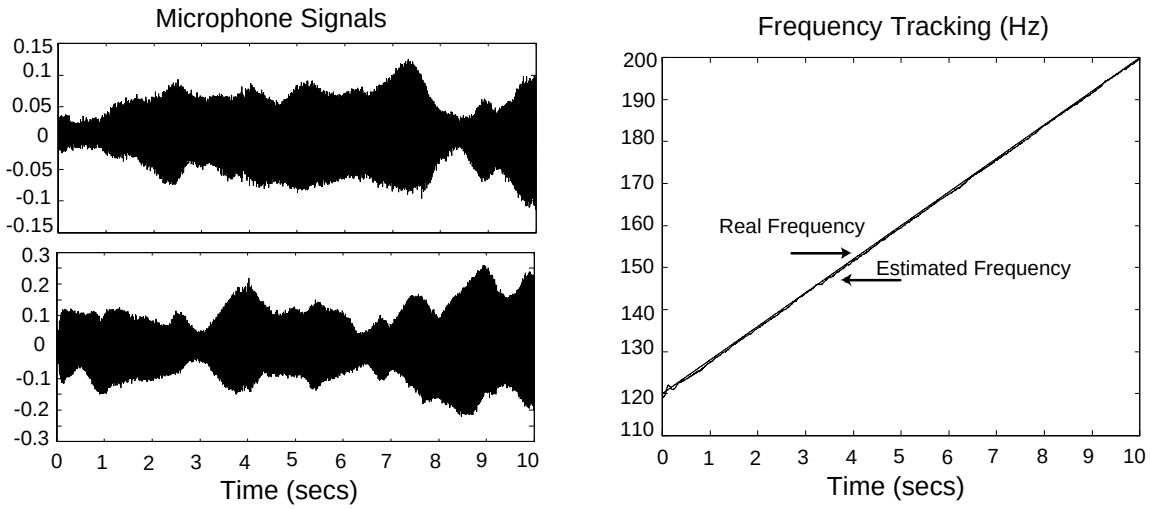

Figure 6: Incoming signals (left) and frequency tracking of the modified estimator (right)

a fundamental component and multiple harmonics. In the basic algorithm, the frequency estimation was based on the fundamental component, although the integer multiplicative relations between the fundamental and harmonics were exploited in the signal reconstruction. The gain K_f improved the dynamic response of the frequency estimation loop and simplified its design. The estimates were unbiased and ripple-free when the signal contained no noise and the parameters of the signal were constant.

A modified version of the algorithm provided improvements for situations in which the fundamental component of the signal could become small, or vanish for some periods of time. In this case, information from all components of the signal were used in the fundamental frequency estimation. Multiple signals with the same fundamental frequency were also combined to yield consistent estimation results despite changes in signal characteristics. In consequence, an advantage of the modified algorithm over the basic algorithm is that it is not necessary to know *a priori* which component is the most suitable to base the frequency estimation on. The algorithms were designed with real-time tracking applications in mind. They were simple in design and implementation, and effective in tracking time-varying parameters. The linear time-invariant approximations gave useful information about the dynamic behavior of the system, the trade-off between convergence speed and noise sensitivity, and the selection of the design parameters.

7. References

[1] S. Bittanti, M. Camp, and S. Savaresi, "Unbiased estimation of a sinusoid in colored noise via adapted notch filters," *Automatica,* vol. 33, no. 2, pp. 209-215, 1997.

[2] S. Bittanti and S. Savaresi, "On the parameterization and design of an extended Kalman filter frequency tracker," *IEEE Trans. Automat. Contr.,* vol. 45, no. 9, pp. 1718-1724, 2000.

[3] M. Bodson, "Performance of an adaptive algorithm for sinusoidal disturbance rejection in high noise," *Automatica*, vol. 37, pp. 1133-1140, 2001.

[4] M. Bodson and S. Douglas, "Adaptive algorithms for the rejection of sinusoidal disturbances with unknown frequency," *Automatica,* vol. 33, no. 12, pp. 2213-2221, 1997.

[5] A. Carlson, *Communications Systems.* New York: McGraw-Hill, 1986.

[6] M. Dragosevic and S. Stankovic, "An adaptive notch filter with improved tracking properties", *IEEE Trans. Signal Processing*, vol.43, no.9, pp. 2068-2078, 1995.

[7] S. Kay and S. Marple, "Spectral analysis—a modern perspective," in *Proc. IEEE,* vol. 69, pp. 1380-1419, 1981.

[8] B. La Scala and R. Bitmead, "Design of an extended Kalman filter frequency tracker," *IEEE Trans. Signal Processing*, vol. 44, no. 3, pp. 739-742, 1996.

[9] G. Li, "A stable and efficient adaptive notch filter for direct frequency estimation," *IEEE Trans. Signal Processing*, vol. 45, no. 8, pp. 2001-2009, 1997.

[10] A. Nehorai, "A minimal parameter adaptive notch filter with constrained poles and zeros," *IEEE Trans. Signal Processing*, vol. 33, no. 4, pp. 983-996, 1985.

[11] D. Rao and S. Kung, "Adaptive notch filtering for the retrieval of sinusoids in noise," *IEEE Trans. Signal Processing*, vol. 32, no. 4, pp. 791-802, 1984.

[12] P. Regalia, "An improved lattice-based adaptive IIR notch filter," *IEEE Trans. Signal Processing*, vol. 39, no. 9, pp. 2124-2128, 1991.

[13] R. Roy and T. Kailath, "ESPRIT—Estimation of Signal Parameters via Rotational Invariance Techniques," *IEEE Trans. Signal Processing*, vol. 37, no. 7, pp. 984-995, 1989.

[14] S. Savaresi, "Funnel filters: A new class of filters for frequency estimation of harmonic signals," *Automatica,* vol. 33, no. 9, pp. 1711-1718, 1997.

[15] J. Stensby, *Phase-Locked Loops: Theory and Applications.* Boca Raton, Fla.: CRC Press, 1997.

[16] P. Strobach, "Fast recursive low-rank linear prediction frequency estimation algorithms," *IEEE Trans. Signal Processing,* vol. 44, no. 4, pp. 834-847, 1996.

[17] B. Wu, *Adaptive Algorithms for Active Control of Periodic Disturbances.* Ph.D. Thesis, Department of Electrical & Computer Engineering, University of Utah, 2002.

[18] B. Wu and M. Bodson, "A magnitude/phase locked loop approach to parameter estimation of periodic signals," in *Proc. of the American Control Conference,* 2001, pp. 3594-3599.

[19] B. Wu and M. Bodson, "Frequency estimation using multiple sources and multiple harmonic components," in *Proc. of the American Control Conference*, 2002, pp. 21-22.